ON THE LOGNORMALITY OF THE SMALL-SCALE STRUCTURE OF TURBULENCE

FRANÇOIS N. FRENKIEL
Naval Ship Research and Development Center, Bethesda, Md. 20084, U.S.A.

and

PHILIP S. KLEBANOFF
National Bureau of Standards, Wash., D.C. 20234, U.S.A.

(Received 15 October, 1974)

Abstract. Higher-order moments of turbulent velocity gradients and their behavior with Reynolds number were measured in the nearly isotropic turbulent field generated by a square-mesh grid and in a turbulent boundary layer along a flat plate with zero pressure gradient. Hot-wire anemometry and instrumentation combining analog and digital methods were used to measure moments up to the fourteenth order. Measurements of such high-order moments required that particular attention be given to their validity. Involved herein was the evaluation of such effects as nonlinearity, averaging intervals, and the adequacy of the statistics for the tails of the probability density distributions. The results obtained are compared with those of other investigators for a variety of flow configurations in the laboratory as well as in the atmosphere. The concept of the intermittency of the small-scale structure and the theoretical approach involving lognormality of the probability density distribution of the dissipation rate are evaluated.

1. Introduction

Although the results obtained by fluid dynamicists in the laboratory have been extensively applied to atmospheric investigations, the converse has not generally been true. The application of high-speed computing to the measurement of turbulence characteristics in both the atmosphere and the laboratory makes it possible for such studies to play a more coordinated role in our understanding of turbulence phenomena. The present paper is concerned with the investigation of the small-scale turbulence structure which is significant in both fluid dynamic and atmospheric turbulence.

The present view of the physical nature of the small-scale turbulence is that it has a spotty or intermittent character in space and time and that decreasing scales are increasingly more intermittent. This intermittent character of a turbulent field can play a major role in many turbulent phenomena such as mixing and chemical kinetics of pollutants in the atmosphere, production of aerodynamic noise, propagation through turbulent media, and other problems involving the nature of the structure of a turbulent field. The concept of small-scale intermittency (which should be distinguished from the intermittencies associated with the outer boundaries of jets, wakes, and boundary layers) was introduced by Batchelor and Townsend (1949) in their studies of grid turbulence at low turbulence Reynolds numbers. A similar concept has been introduced in both theoretical and experimental studies of atmospheric turbulence for which, because of the higher Reynolds number, such concepts are considered more applicable. Kolmogoroff (1962) and Obukhov (1962) took intermittency into account by considering the spatial randomness of dissipation which led

Boundary-Layer Meteorology **8** (1975) 173–200.

to a modification of their earlier theories of turbulence. Yaglom (1966) and Gurvich and Yaglom (1967) extended these ideas leading to log-normal probability distributions for the fluctuations of the rate of energy dissipation giving a statistical model characterizing the physical process of a cascade-breakdown of turbulent eddies. These concepts involve the need for information about the statistical properties of turbulent velocity gradients and more particularly about the relations for higher-order moments and their behavior with Reynolds number. The energy dissipation rate is given by

$$\varepsilon = \tfrac{1}{2}\nu\left(\frac{\partial u_i}{\partial x_j} + \frac{\partial u_j}{\partial x_i}\right)^2$$

which would involve the measurements of a complex combination of nine derivatives of spatial gradients of turbulent velocity components all of which, in the present state of the art, are not measurable. However, as have other investigators, it is assumed that a representative measure of the dissipation is obtained by measuring $(\partial u/\partial t)^2$ involving the assumption of isotropy and Taylor's assumption of space-time equivalence. Obtaining reliable data on the behavior of high-order moments of velocity gradients in a turbulent field, particularly for the atmosphere, presents difficult problems of measurement (Tennekes and Wyngaard, 1972). For the atmosphere, such measurements have been limited to the fourth-order moments which, apart from the large scatter they exhibit, are not of sufficiently high-order to permit an evaluation of the type attempted in the present paper. On the other hand, in the laboratory, higher-order moments for both velocity and velocity-gradients have been measured (Frenkiel and Klebanoff, 1967, 1971, 1973; Van Atta and Chen, 1968).

In this paper an effort is made to evaluate the afore-mentioned concepts by experimental studies of the turbulence downstream of a grid and in the boundary layer. Some of the early measurements of wind-tunnel turbulence using high-speed digital computing methods (Frenkiel, 1952) indicated the importance of the use of sufficiently long sample-recordings of data, which in turn required much more advanced computer facilities than were then available. Such measurements were further advanced in 1965 using more appropriate computer facilities and some results were reported using a 12.5-s sample recording digitized at a rate of 12800 sample-points per second (Frenkiel and Klebanoff, 1965). In the present paper, the measurement of higher-order moments of turbulent velocity gradients, which are substantially higher than the fourth-order moments, impose severe requirements involving many millions of sample-points, and considerable attention is given to the validity of such measurements. The results obtained are compared with those by others for the atmospheric boundary layer and in the laboratory using various flow configurations.

2. Experimental Procedure and High-Speed Computing Methods

The investigation was carried out in the nearly isotropic turbulence field generated by a square-mesh grid woven of iron rods, 0.5 cm in diam, and a mesh of 2.54 cm

and in a turbulent boundary layer along a flat plate with zero-pressure gradient.

Both the grid and boundary-layer measurements were performed in the test section of the 1.37-m wind tunnel at the National Bureau of Standards. The grid was placed perpendicular to the flow at the beginning of the test section and the measurements presented in this paper were made at 48.5 mesh lengths downstream of the grid at wind velocities, U_1, of 7.6 and 15.3 m s^{-1}. The turbulent boundary-layer (with the turbulence grid removed) was established on an aluminum plate 3.66 m long which was mounted vertically and centrally in the tunnel. A false wall mounted on the tunnel wall opposite the working side of the plate was adjusted to give a zero-pressure gradient along the plate. The pressure distribution was determined by means of a static tube mounted on a carriage that could be moved and positioned from outside the tunnel. The first 0.61 m of the plate was covered with No. 16 floor-sanding paper to increase the thickness of the boundary-layer (Klebanoff and Diehl, 1951).

Measurements were made in the boundary-layer at 3.2 m from the leading edge and at free-stream velocities of about 3.8, 7.5–7.8, and 15.3 m s^{-1}, for which the boundary-layer thickness δ ranged from about 7.4 to 8.1 cm. Since all the measurements were made at the 3.2-m station, the measuring probe was supported by a rod extending through the plate to a 0.634-mm (0.025 in) micrometer screw traversing device mounted on the non-working side of the plate, and remotely controlled from outside the tunnel. The initial distance from the surface was obtained by using a prism to reflect the images of the surface and the probe on the calibrated scale of a microscope.

Instrumentation combining analog and digital methods, similar to that described previously (Frenkiel and Klebanoff, 1967), was used. Most of the data were obtained using constant-current hot-wire anemometry. Generally, the hot-wires were platinum wires 1.25 μm in diam and 0.32 and 0.7 mm in length. Wires 0.63 μm in diam and 0.16 mm in length were also used. This permitted an evaluation of the effect of wire length, l, on the measurements. No corrections for the nonlinear response of the constant current hot-wire have been made to the data given in the present paper. An estimate of the effect of the nonlinear response on the moments of the velocity derivatives up to the fourteenth order was made for some of the boundary-layer data using linearized constant temperature hot-wire equipment. The effect was found to be not very significant for even-order moments within the experimental dispersion.

The fluctuating voltages corresponding to the temporal gradient of the longitudinal component of the turbulent velocity, $\partial u/\partial t$, were recorded on magnetic tape, at a tape speed of 152.4 cm s^{-1} using an Ampex FR-1300* multichannel tape recorder. Timing signals of 12800 and 25600 Hz were recorded simultaneously. The differentiation was accomplished using an operational amplifier in the differentiating mode for which the departure from linearity with frequency was 1% at 10000 Hz and 4% at 20000 Hz. To improve the signal-to-noise characteristics, a low-pass electronic filter was used with varying cut-off frequencies, f_c. However, there are restrictions imposed on f_c by the requirement to include all the frequencies of interest and by the signal-to-noise ratio.

* Brand names of equipment are used solely to provide a reference for performance characteristics and do not represent an endorsement.

TABLE I

Frequency response data

(a) Constant current hot-wire							
Cut-off frequency f_c, kHz	3.5	4	6	8	10	12	20
Relative amplification (at f_c)	0.83	0.81	0.78	0.82	0.81	0.78	0.72
(b) Linearized hot-wire							
Cut-off frequency f_c, kHz	5.5	15.5–18.5					
Relative amplification (at f_c)	0.84	0.82					

The various values of cut-off frequency which were used and the amount by which the frequency response is down at the cut-off frequency are given in Table I. This amount is not constant and appears to vary inconsistently. This is because it incorporates the frequency response of a variable filter in the hot-wire amplifier and the frequency response of the differentiating circuit in addition to that of the low-pass filter.

The analog tapes were digitized and the digital tapes processed using the computer facilities of the Computation and Mathematics Department at the Naval Ship Research and Development Center. The analog data were digitized at a rate of about twice the cut-off frequencies yielding sample-recordings of digitized data corresponding to about 12.5 s of analog recording. Thus, the number of individual points for which the instantaneous turbulent velocity gradient values were used in the analysis varied from 90000 to 500000 per sample-recording depending on the digitizing rate selected. In most cases more than one sample-recording was used to determine the turbulent characteristics for the data measured under the same general conditions. The gain used during digitizing was adjusted to cover the full range of the fluctuating voltage e and of its gradient $\partial e/\partial t$ over an appreciable number of standard deviations $\sqrt{\overline{e^2}}$ and $\sqrt{\overline{(\partial e/\partial t)^2}}$, respectively. At the same time attention was given to minimizing any possible errors from fluctuations in voltage extending outside of the range of the digitizer. For the data used in the present paper the range varied from 4.2 to $9.0\sqrt{\overline{e^2}}$ for the voltage and from 7.3 to 28.1 $\sqrt{\overline{(\partial e/\partial t)^2}}$ for the derivative of the voltage.

Data pertaining to the calibration of the hot-wire amplifier and to the noise were also recorded and digitized. The digitized data were plotted and inspected to determine any obvious interference with meaningful turbulence data or improper operation of the recorder or digitizer.

3. Higher-Order Moments of Turbulent Velocity Gradients

The higher-order moments,

$$\overline{v_t^{2n}} = \frac{\overline{(\partial u/\partial t)^{2n}}}{[\overline{(\partial u/\partial t)^2}]^n}, \tag{1}$$

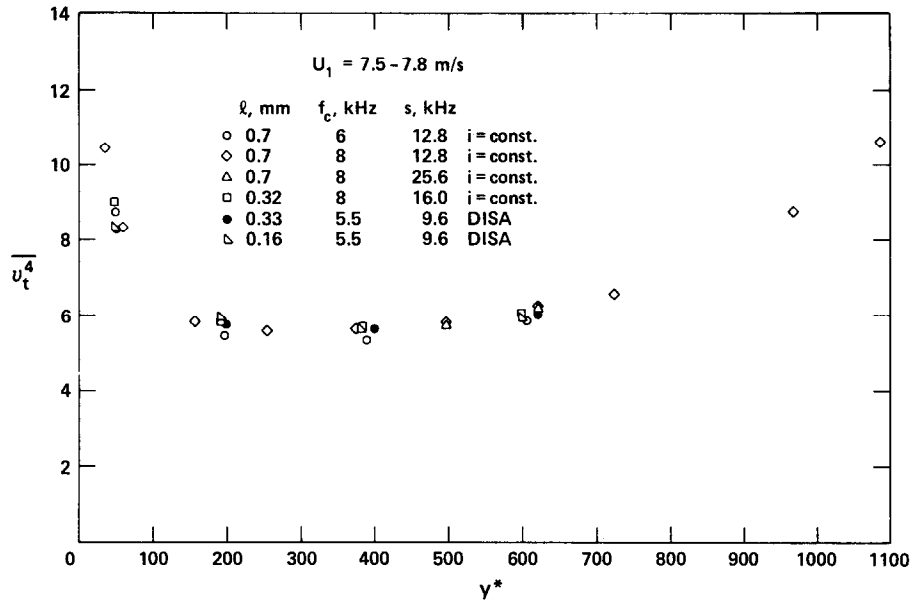

Fig. 1. Fourth-order moments for the gradient of the longitudinal turbulent velocity component in the boundary-layer at a free-stream velocity 7.5 to 7.8 m s^{-1}.

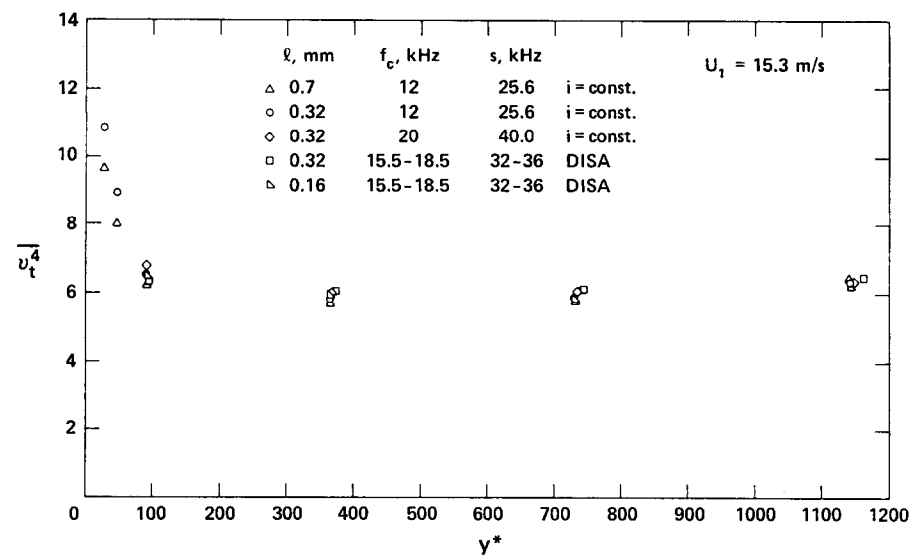

Fig. 2. Same as for Figure 1, but at a free-stream velocity of 15.3 m s^{-1}.

were determined for both grid and boundary layer turbulence. Figures 1 and 2 present the values of the fourth moment, $\overline{v_t^4}$, in the boundary-layer for varying distance y from the wall at free-stream velocities of 7.5–7.8 and 15.3 m s^{-1}, respectively. The distance from the wall is represented non-dimensionally as $y^* = u_\tau y/\nu$, where u_τ is

the wall friction velocity and ν is the kinematic viscosity. The values of u_τ at the different free-stream velocities were obtained by fitting the logarithmic law (Kline *et al.*, 1969)

$$u^* = \frac{U}{u_\tau} = 5.0 + 5.6 \log_{10} y^*$$

to the measured distributions of mean velocity U.

The selected frequency response and wire length of the hot wire, in particular as they relate to the measurement of derivatives, are always important considerations and at best represent a compromise between frequency response and the ratio of signal to noise. Figures 1 and 2 illustrate the effect of these variables on the experimental measurements at two different mean velocities. These show the measurements of $\overline{v_t^4}$ for three different cut-off frequencies and three different wire lengths, as well as a comparison between data obtained by constant current hot-wire equipment (i=const) and the linearized constant temperature equipment (DISA). At the higher mean wind speed, higher cut-off frequencies were used, since the turbulence frequencies increase accordingly. For the selected cut-off frequencies and wire lengths the differences are small for the measurements of the fourth-order moments except close to the surface for the higher free-stream velocity, where much smaller turbulence scales are present. The wire length was selected as short as practical compared with the Kolmogoroff length (see Wyngaard, 1968) insuring that an adequate response would be obtained. Figure 1 also includes a comparison of values of $\overline{v_t^4}$ obtained from the same sample-recording of data using two different digitizing rates (s=12.8 and 25.6 kHz for f_c=8 kHz and l=0.7 mm). The results are almost identical.

The data of Figures 1 and 2, except for those corresponding to the wire length

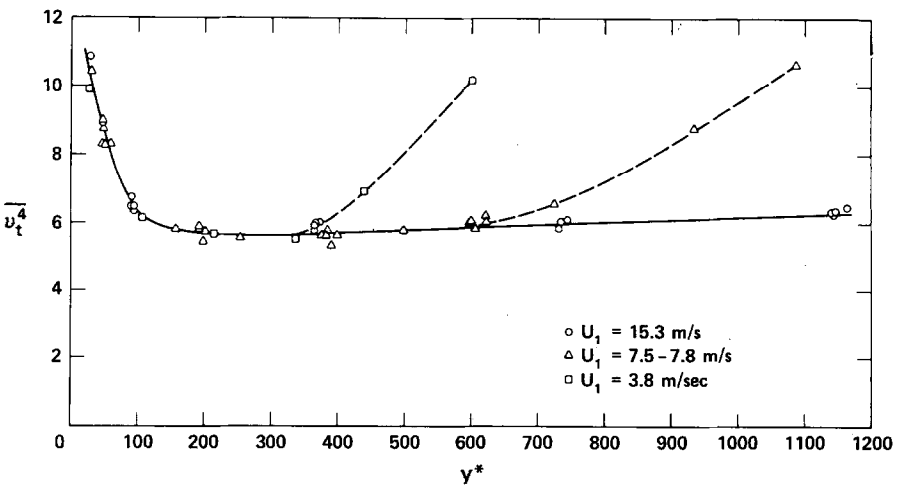

Fig. 3. Comparison of fourth-order moments in the boundary-layer for different free-stream velocities.

$l=0.7$ mm at $U_1=15.3$ m s^{-1}, are replotted in Figure 3 together with additional data for $\overline{v_t^4}$ obtained at $U_1=3.8$ m s^{-1}. The data for this lower free-stream velocity were obtained for $l=0.7$ mm with $f_c=4$ kHz and $s=12.8$ kHz except at $y=0.8$ ($y^*=335$) for which $s=8$ kHz. The number of sample-recordings used to obtain each experimental point shown on Figures 1 to 3 ranged from 1 to 10; however, no distinction has been made as to the number of sample-recordings since the dispersion in the values of $\overline{v_t^4}$ was small. For subsequent data involving moments of higher order than the fourth, where the dispersion may be significant, only averages over a number of sample-recordings are used. The figures show that there is a strong variation of $\overline{v_t^4}$ with distance from the surface. For a proper evaluation of the concept of the intermittency of the small-scale structure, as well as for comparison with other investigators, it is desirable to avoid the influence of the surface. It is also necessary to avoid a different type of intermittency, characteristic of the outer region of the turbulent layer, which affects the fourth-order moment $\overline{v_t^4}$ as shown by the dashed curves in Figure 3. Values of y^* of 340, 600, and 1100 for $U_1=3.8$, 7.5–7.8, and 15.3 m s^{-1}, respectively, correspond to y/δ of about 0.4 at which position the intermittency of the outer region is considered to begin (Klebanoff, 1954; Corrsin and Kistler, 1954). In the inner region of the boundary-layer, meaning at y/δ less than 0.4, the fourth-order moments scale reasonably well with y^*. The region of the boundary-layer of particular interest in the present study is that where $\overline{v_t^4}$ is fairly constant extending from y^* of about 150 to y/δ of about 0.4. The wire lengths, cut-off frequencies, and other pertinent data for the measurements obtained by the present authors for this region in the boundary-layer and for grid turbulence are given in Table II. As suggested by Kuo and Corrsin (1971), f_c for these measurements was selected so as to be of the order of the Kolmogoroff frequency, $f^*=U/2\pi\eta$ [where $\eta=(\nu^3/\varepsilon)^{1/4}$ is the Kolmogoroff scale with ε being the rate of dissipation per unit mass]. The values listed for the Kolmogoroff scale η and Kolmogoroff frequency f^* assume an isotropic relation for the rate of dissipation which leads to the relation

$$\eta=(15)^{-1/4}\frac{\lambda}{R_\lambda^{1/2}}, \tag{2}$$

where λ is the Taylor microscale and $R_\lambda=\sqrt{\overline{u^2}}\lambda/\nu$. The ratios l/η vary from 0.86 to 3.2 and Figures 1 to 3 indicate that these ratios should be adequate.

An important question related to the concept of intermittency of the small-scale structure has been the dependence of $\overline{v_t^4}$ on the turbulence Reynolds number R_λ. Figure 4 shows the variation of $\overline{v_t^4}$ with R_λ for the present investigation together with the results of other investigations for several types of flow configurations in the laboratory (Batchelor and Townsend, 1949; Comte-Bellot, 1965; Wygnanski and Fiedler, 1970; Wyngaard and Tennekes, 1970; Kuo and Corrsin, 1971; Antonia, 1973) and in the atmosphere (Pond and Stewart, 1965; Gibson *et al.*, 1970; Wyngaard and Tennekes, 1970; Sheih *et al.*, 1971).

TABLE II

Experimental conditions

	U_1 m s^{-1}	y mm	R_λ	l mm	f_c kHz	s kHz	f^* kHz	$\frac{l}{\eta}$	y^*	Number of sample recordings	Number of points per sample	Hot-wire equipment
Grid turbulence	7.6	–	39	0.32	3.5	7	3.4	0.86	–	11	90000	i=const.
	15.3	–	59	0.32	10	20	11.7	1.5	–	11	250000	i=const.
Boundary-layer	3.8	31.8	91	0.70	4	8	1.6	2.2	335	5	100000	i=const.
	7.8	20.3	151	0.32	8	16	5.5	1.8	383	5	200000	i=const.
	7.8	10.2	142	0.32	8	16	5.6	2.0	191	4	200000	i=const.
	15.3	10.2	196	0.32	20	40	17.4	3.2	367	10	500000	i=const.
	15.3	20.3	213	0.32	20	40	16.9	2.8	733	10	500000	i=const.
	15.3	20.3	213	0.32	16.5	32	17.1	2.8	743	8	400000	DISA
	7.5	10.2	143	0.32	5.5	9.6	5.5	2.1	199	4	120000	DISA
	7.5	20.3	152	0.32	5.5	9.6	5.4	1.8	398	4	120000	DISA
	7.7	20.3	149	0.16	5.5	9.6	5.5	0.9	382	4	120000	DISA

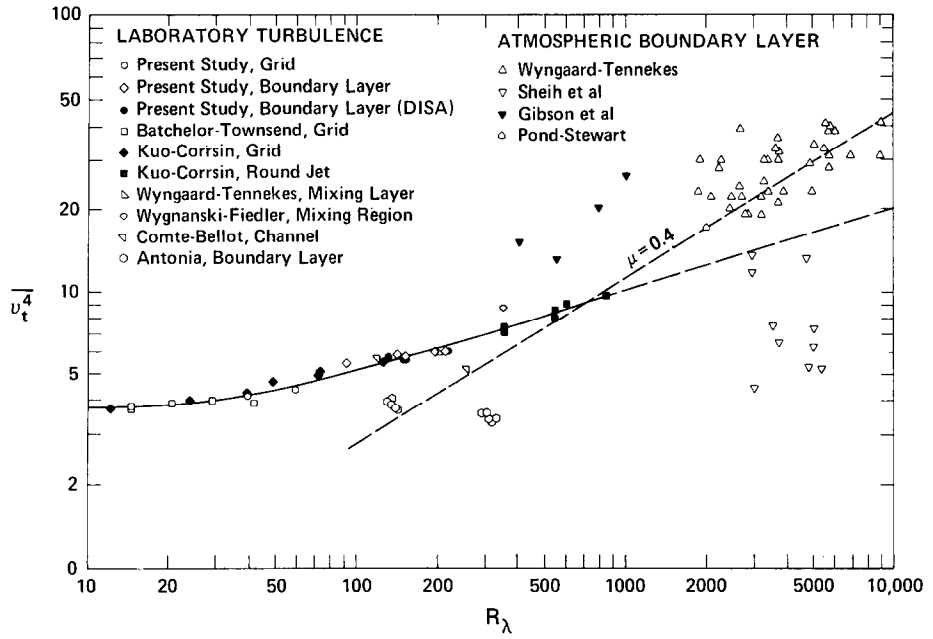

Fig. 4. Variation of fourth-order moments with the Reynolds number of turbulence.

In the present study, R_λ is given as $\sqrt{\overline{u^2}}\,\lambda/\nu$ where $u(t)$ is the longitudinal component of the turbulent velocity and

$$\lambda^2 = [\overline{u^2}/\overline{(\partial u/\partial t)^2}]U^2. \tag{3}$$

In an isotropic field of turbulence and assuming the equivalence of space-time (Taylor's assumption) the above relation for λ corresponds to that for the Taylor microscale. In general, however, for nonisotropic flows, there is some ambiguity in the definition for R_λ. It was desirable, therefore, wherever possible, in order to be consistent for the purpose of comparison, that values of R_λ for different investigations be presented in a similar manner. For the most part, the R_λ shown in Figure 4 was obtained according to Equation (3). However, for the data of Gibson *et al.* (1970) R_λ was estimated by the authors (private communication) from the relation $R_\lambda = 0.48\,(Uy/\nu)^{1/2}$. The R_λ for the single point of Pond and Stewart is that estimated by Sheih *et al.* (1971) and values of R_λ for the atmospheric data of Wyngaard and Tennekes (1970) used the vertical component of the turbulent velocity instead of the longitudinal component; however, λ was obtained using Equation (3).

It should be noted that there is relatively small scatter for the values of $\overline{v_t^4}$ for the various laboratory measurements as compared to the atmospheric data. In general, the laboratory data, with perhaps the exception of the data of Antonia, support the view of a certain universality of structure for small-scale turbulence. In fact, the atmospheric data, within their scatter, are consistent with the extrapolation of the laboratory data. However, the manner in which this extrapolation should be made is

uncertain. Corrsin (1962) and Tennekes (1968) have proposed some simple models of the intermittency of small-scale structure which indicate that $\overline{v_t^4}$ is proportional to $R_\lambda^{1.5}$ and R_λ, respectively. The data presented in Figure 4 indicate a smaller variation with R_λ than do either of these models, an observation which has already been noted by other investigators (Wyngaard and Tennekes, 1970; Gurvich and Zubkovskii, 1963). The expected dependence of $\overline{v_t^4}$ on Reynolds number can be seen from the hypothesis (Kolmogoroff, 1962; Obukhov, 1962) that the variance of the logarithm of the locally averaged dissipation is given by

$$\sigma^2 = A(\mathbf{x}, t) + \mu \ln(L/r), \tag{4}$$

where L is a macroscale of turbulence, r is a characteristic dimension of the averaging volume, $A(\mathbf{x}, t)$ depends on the nature of the very large-scale structure, and μ is a universal constant. If it is assumed that $r \sim \eta$, where η is the Kolmogoroff microscale, $L/\eta \propto R_\lambda^{3/2}$. At very large Reynolds numbers, for which $A(\mathbf{x}, t)$ can be neglected,

$$\sigma^2 = \mu \ln R_\lambda^{3/2}. \tag{5}$$

For a log-normal probability distribution $\sigma^2 = \ln \overline{v_t^4}$, and with this assumption

$$\overline{v_t^4} = R_\lambda^{(3/2)\mu}. \tag{6}$$

For higher-order moments, the Gurvich and Yaglom (1967) model can be generalized to give

$$\overline{v_t^{2n}} \propto R_\lambda^{(3/4)\mu n(n-1)}. \tag{7}$$

Attempts to determine the Reynolds number dependence of $\overline{v_t^4}$, i.e., $\overline{v_t^4} \propto R_\lambda^m$, have yielded, either from direct measurement of $\overline{v_t^4}$ or from the slope of the spectrum of $(\partial u/\partial t)^2$, values of m ranging from 0.13 to 0.85 (Pond and Stewart, 1965; Gibson *et al.*, 1970; Stewart *et al.*, 1970).

Using the data from the present study, giving higher-order moments $\overline{v_t^{2n}}$, a direct evaluation of Equation (7) is presented in Figure 5. In this figure $\log_{10} \overline{v_t^{2n}}$ (for $n = 2$, 3, and 4) for grid and boundary-layer turbulence from the present investigation are presented as a function of $n(n-1) \log_{10} R_\lambda$. In addition, comparison is made with some of the data which are available for $n = 2$ from investigations in the atmosphere. Gurvich and Yaglom (1967) proposed the value of 0.4 for μ, which was obtained from spectral measurements in the atmosphere of $(\partial w/\partial t)^2$ made by Gurvich and Zubkovskii (1963) and of $(\partial u/\partial t)^2$ made by Pond and Stewart (1965). This oft-quoted value is shown in Figures 4 and 5. Also shown in Figure 4 is an extrapolation of laboratory data as inferred from the behavior in Figure 5. This extrapolation considers the possibility that the atmospheric data are consistent with the trend of the higher-order moments as obtained in the laboratory and as shown in Figure 5. In this connection it should be noted, in view of the trend with distance from the surface shown in Figures 1 to 3, that the atmospheric data reported by Wyngaard and Tennekes (1970) were measured at 5.6, 11.3, and 22.6 m above the ground, while that of Sheih *et al.* (1971) were measured 108 m above the ground. The measurements of Gibson *et al.* (1970) over the open ocean were made at heights from 2.3 to 11.6 m. In addition,

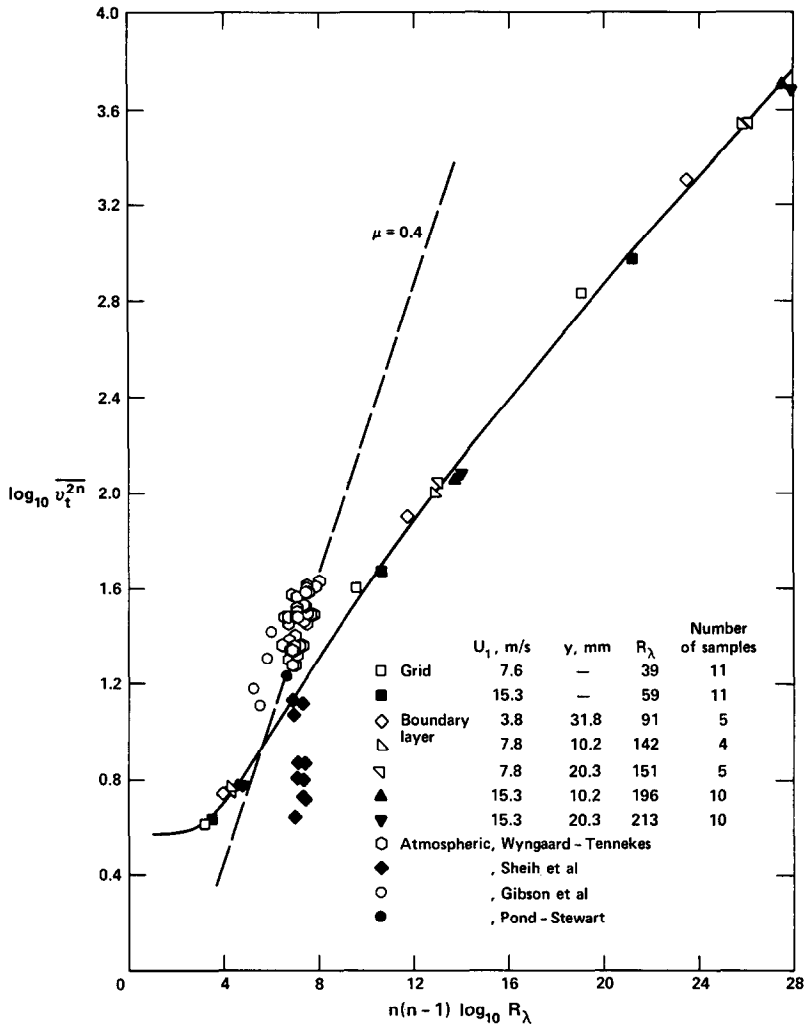

Fig. 5. Comparison of measured moments up to eighth-order in a form suggested by lognormality.

the possibility of dust and water drops affecting the atmospheric measurements and resulting in values for $\overline{v_t^4}$ which are too high, cannot be completely discounted. On the other hand, the data by Sheih *et al.* (1971) may be too low due to an overloaded signal (Lumley, private communication). Thus, it is reasonable to infer, from Figure 5, that the atmospheric data are consistent with the trend exhibited by the higher order moments measured in the laboratory. It is also reasonable to infer that the deviation from Equation (7) and the fact that μ is not constant are not due to an insufficiently large Reynolds number. However, apart from the question of the Reynolds number in the comparison between experiments and theory, there is also the consideration, referred to later, of the appropriate size of the averaging volumes over which the measurements of $(\partial u/\partial t)^2$ should be made.

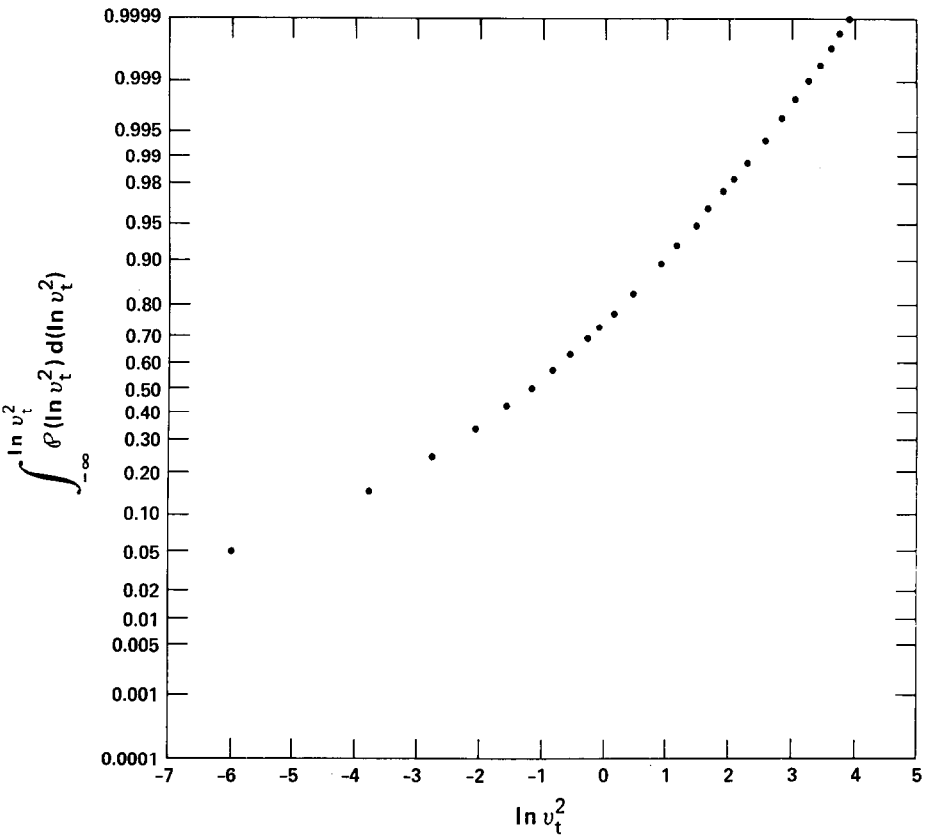

Fig. 6. Cumulative probability density distribution of $\ln v_t^2$.

Figure 6 presents the cumulative probability density distribution of $\ln v_t^2$ for the averages from 10 sample-recordings obtained with the constant current hot-wire at $y = 20.3$ mm and $U_1 = 15.3$ m s^{-1}. In this figure a log-normal distribution would be represented by a straight line, and it is clearly evident that such is not the case. However, it is interesting that the data of Figure 5 appear to correlate in a form suggested by Gurvich and Yaglom but not as required by log-normality of the distribution of energy dissipation; i.e., if one considers the Reynolds numbers to be sufficiently high for Equation (7) to be valid, then μ does not appear to be constant but varies with the order of the moment $2n$ or the Reynolds number R_λ. In fact, the measured eighth-order moments shown in Figure 5 evidence a significant departure from a constant μ which does not appear to be due to experimental scatter. This is of some interest from a theoretical point of view, for as shown by Orszag (1970), the log-normal distribution of energy dissipation is inconsistent with theories of turbulence in terms of moments.

In order to assess the reality of the departure from a constant μ, some measurements of higher-order moments up to $2n = 14$ were made and these are presented in Figure 7. The departure from a constant μ is clearly evident and, perhaps more important, the

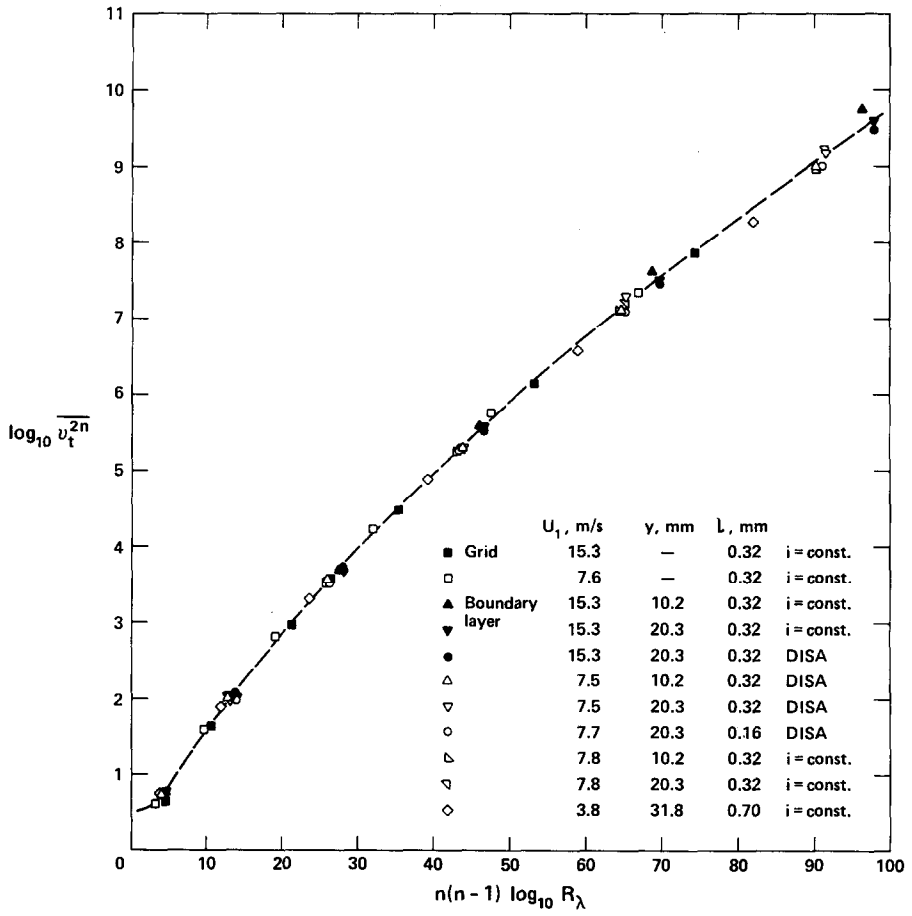

Fig. 7. Comparison of measured higher-order moments up to fourteenth order in a form suggested by lognormality.

consistency of the data defining a general curve is maintained. This consistency may be significant since it indicates that even for the higher-order moments of velocity gradients the measurements in a grid-produced turbulence and in the boundary-layer compare very well. Also, the measurements obtained using linearized constant temperature hot-wire equipment compare well with those obtained using constant current equipment thus confirming that the measurements of even-order moments of gradients of turbulent velocities are not significantly affected by nonlinearization.

4. Validity of Higher-Order Moments

The higher-order moments $\overline{v_t^{2n}}$ were determined by directly computing the averages of the individual (digitized) values of $\overline{v_t^{2n}}$ according to Equation (1). However, it

should be noted that the validity of the moments $\overline{v_t^{2n}}$ obtained in this manner depends on how well the relation

$$\overline{(\partial u/\partial t)^{2n}} = \int_{-\infty}^{+\infty} (\partial u/\partial t)^{2n}\, p(\partial u/\partial t)\, d(\partial u/\partial t), \tag{8}$$

where $p(\partial u/\partial t)$ is the probability density distribution of $\partial u/\partial t$, is satisfied, i.e., the accuracy of such measures requires the closure of the tails of the probability density distribution $p(\partial u/\partial t)$ for $(\partial u/\partial t)^{2n} p(\partial u/\partial t)$ at increasing $\partial u/\partial t$. With the nondimensional coordinates $v_t = (\partial u/\partial t)/\sqrt{\overline{(\partial u/\partial t)^2}}$ and

$$\mathscr{P}(v_t) = \sqrt{\overline{\left(\frac{\partial u}{\partial t}\right)^2}}\, p\left(\frac{\partial u}{\partial t}\right) d\left(\frac{\partial u}{\partial t}\right)$$

we find

$$\int_{-\infty}^{+\infty} p\left(\frac{\partial u}{\partial t}\right) d\left(\frac{\partial u}{\partial t}\right) = \int_{-\infty}^{+\infty} \mathscr{P}(v_t)\, \mathrm{d}v_t = 1$$

with

$$\overline{v_t^2} = \int_{-\infty}^{+\infty} v_t^2 \mathscr{P}(v_t)\, \mathrm{d}v_t = 1 \tag{9}$$

and Equation (8) replaced by

$$\overline{v_t^{2n}} = \int_{-\infty}^{+\infty} v_t^{2n} \mathscr{P}(v_t)\, \mathrm{d}v_t . \tag{10}$$

The validity of moments similar to $\overline{v_t^{2n}}$, but for the turbulent velocities (rather than for gradients of turbulent velocities), has been discussed in a previous paper (Frenkiel and Klebanoff, 1973). In that case higher-order moments up to $2n = 8$ were measured with both even and odd moments, and it has been noted that a relation similar to Equation (10) is satisfied. However, in the present case the fluctuating gradients of turbulent velocities are of much higher frequency and higher amplitudes (measured in standard deviations) than the fluctuating turbulent velocities and the measurements are made up to the fourteenth order. In fact, it was shown that for the atmospheric turbulence, condition (10) cannot easily be satisfied for the moments of turbulent velocity gradients higher than the fourth-order by the usual techniques (Tennekes and Wyngaard, 1972).

The main difficulty in determining the probability distribution of the fluctuating derivatives of turbulent velocities is that they extend over a large number of standard-deviations $\sqrt{\overline{v_t^2}}$. In order to improve the precision of the measurements of the probabil-

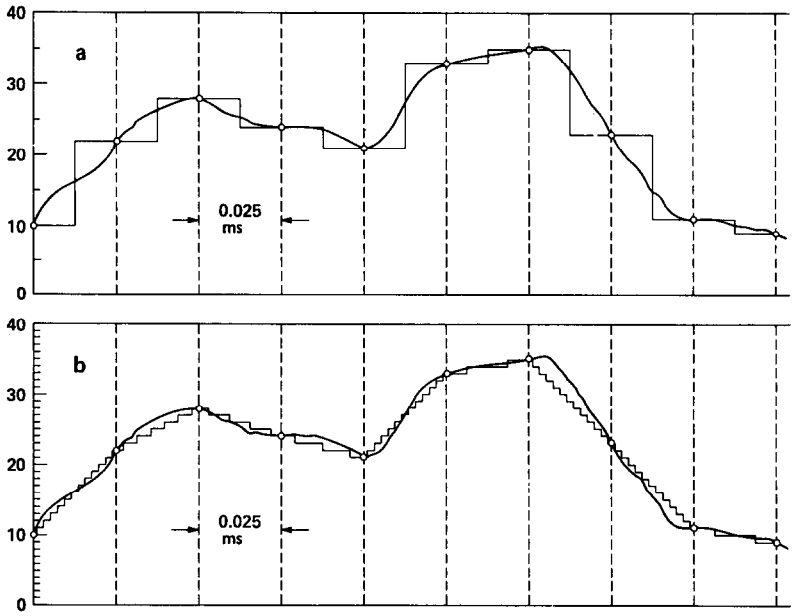

Fig. 8. Schematic representation of interpolation procedure.

ity distribution, a large number of sample-recordings and a high-digitizing rate are desirable; however, this would be inordinately expensive. In order to determine the validity of the measurements of higher-order moments $\overline{v_t^{2n}}$ up to $2n=14$ in the present study, a new method of analysis was used to improve an estimate of the probability distribution as it relates to the question of closure for the integrands $v_t^{2n}\mathscr{P}(v_t)$ at increasing values of v_t in Equation (10). This method is illustrated in Figure 8. In this figure the fluctuating signal is illustrated with the usual digitizing procedure shown in Figure 8(a) where the signal is approximated in a stepwise manner as determined by the digitizing rate (illustrated in the figure to be about 40 kHz) and the ordinates represent the digitized values which vary within the range between -1024 and $+1024$, of the fluctuating voltage. An interpolation [see Figure 8(b)] is produced by dividing the intervals between digitized points into steps corresponding to consecutive integer values within each interval, resulting in a considerably increased number of individual data-points. It should be noted that such a procedure will introduce a bias in that the signal is now approximated by linear segments joining successive digitized values. The rate of digitizing is close to twice the cut-off frequency and thus an increase in the digitizing rate would not provide much additional information about the statistical characteristics of the signal although it would reduce the bias.

Figure 9 illustrates the values of nondimensional gradients of velocity $v_t=v_i$ and $v_t=v_{i+1}$ corresponding to two succeeding digital measurements A and B at times t_A and t_B separated by a time interval Δt. We will assume that the stepwise function is

approximated by the line AB and will find that at time $t_A+\kappa$ the nondimensional velocity gradient is equal to

$$v_{i,z} = v_i + z(v_{i+1} - v_i), \tag{11}$$

where

$$z = \kappa/\Delta t$$

and $0 \leqslant z \leqslant 1$. For the square of the velocity gradients averaged over the time interval Δt, we obtain

$$v_*^2 = \int_0^1 v_{i,z}^2 \, dz = \tfrac{1}{3}v_{i+1}^2 + \tfrac{1}{3}v_i^2 + \tfrac{1}{3}v_i v_{i+1}.$$

Averaging over a large number N of intervals Δt we obtain a value for the second moment

$$\overline{v_*^2} = \overline{\int_0^1 v_{i,z}^2 \, dz} = \tfrac{1}{3}(\overline{v_{i+1}^2} + \overline{v_i^2} + \overline{v_i v_{i+1}}).$$

Thus, noting Equation (9) and that by definition $\overline{v_t^2} = 1$, the interpolation represented in Figure 8(b) will lead to

$$\overline{v_*^2} = \tfrac{2}{3}\overline{v_t^2} + \tfrac{1}{3}\overline{v_t(t)\, v_t(t+\Delta t)} = \tfrac{2}{3} + \tfrac{1}{3}\overline{v_t(t)\, v_t(t+\Delta t)} \tag{12}$$

and, in general, $\overline{v_*^2} \neq 1$.

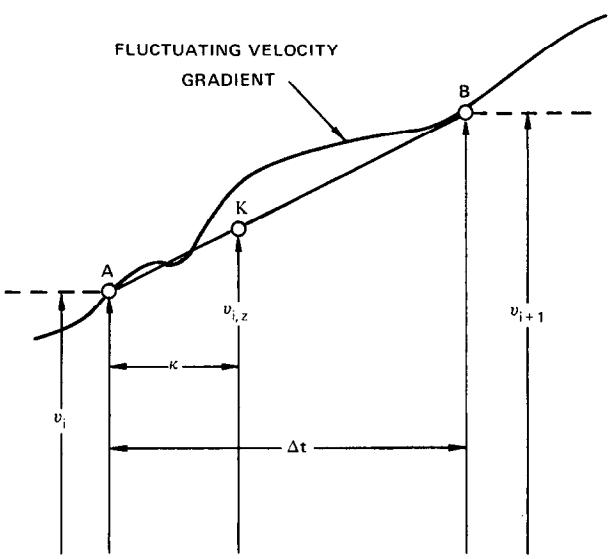

Fig. 9. Illustration of linear interpolation between successive digital measurements.

In a similar manner we find

$$\overline{v_*^m} = \int_0^1 v_{i,z}^m \, dz = \frac{1}{m+1} [v_i^m + v_i^{m-1} v_{i+1} + v_i^{m-2} v_{i+1}^2 + \cdots + v_i v_{i+1}^{m-1} + v_{i+1}^m],$$

and, noting that $\overline{v_t^m(t)} = \overline{v_t^m(t+\Delta t)}$,

$$\overline{v_*^m} = \frac{1}{m+1} [\overline{2v_t^m} + \overline{v_t^{m-1}(t)\, v_t(t+\Delta t)} + \\ + \overline{v_t^{m-2}(t)\, v_t^2(t+\Delta t)} + \cdots + \overline{v_t(t)\, v_t^{m-1}(t+\Delta t)}] \tag{13}$$

or

$$\overline{v_*^m} = \frac{1}{m+1} \left[\overline{\frac{v_t^{m+1}(t+\Delta t) - v_t^{m+1}(t)}{v_t(t+\Delta t) - v_t(t)}} \right]. \tag{14}$$

Let us now define a probability distribution $\mathscr{P}_*(v_t)$ such that

$$\overline{v_*^{2n}} = \int_{-\infty}^{+\infty} v_t^{2n} \mathscr{P}_*(v_t) \, dv_t. \tag{15}$$

$\mathscr{P}_*$ will represent the density distribution of the fluctuating values of $v_{i,z}$, as defined by Equation (11), but expressed as a function of v_t. It should be noted that, in general, $\overline{v_*^{2n}} \neq \overline{v_t^{2n}}$.

The effect that the interpolation between the digitized data, referred to above, has on the resulting probability distribution is shown in Figure 10 where the probability distribution $\mathscr{P}_*(v_t)$ is compared to $\mathscr{P}(v_t)$ for the average from 10 sample-recordings obtained with the constant current hot-wire at $y = 20.3$ mm and $U_1 = 15.3$ m s^{-1}. The figure illustrates that the probability distribution $\mathscr{P}_*(v_t)$ has much less scatter for higher values of v_t than the distribution $\mathscr{P}(v_t)$ and therefore, will permit a more adequate evaluation of the closure of such probability distributions as they relate to the measurements of higher-order moments.

With the definitions

$$\mathscr{P}^\dagger(v_t) = \mathscr{P}(+v_t) + \mathscr{P}(-v_t) \tag{16}$$

and

$$\mathscr{P}^*(v_t) = \mathscr{P}_*(+v_t) + \mathscr{P}_*(-v_t), \tag{17}$$

$$\overline{v_t^{2n}} = \int_0^\infty v_t^{2n} \mathscr{P}^\dagger(v_t) \, dv_t \tag{18}$$

and

$$\overline{v_*^{2n}} = \int_0^\infty v_t^{2n} \mathscr{P}^*(v_t) \, dv_t. \tag{19}$$

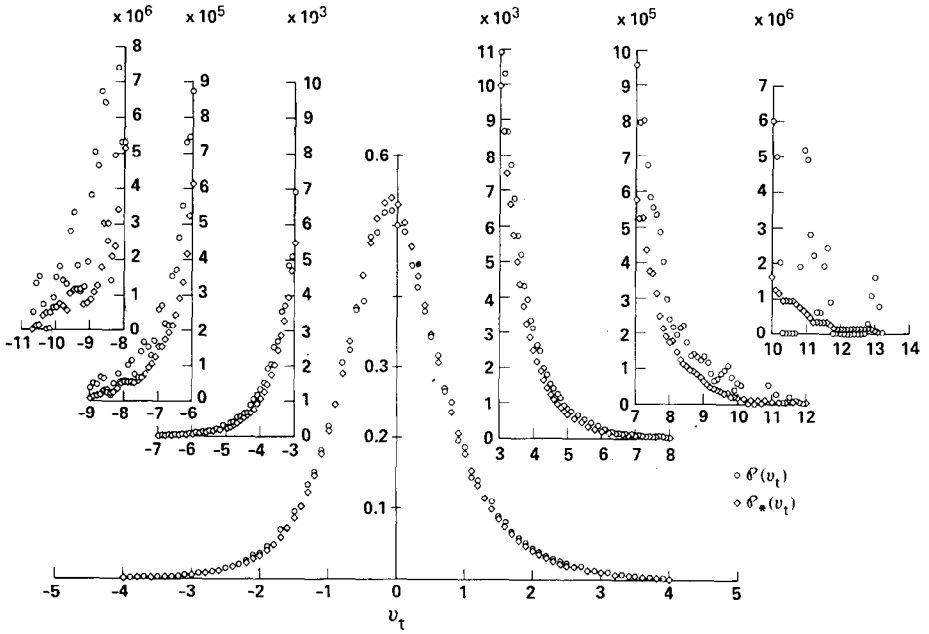

Fig. 10. Comparison of interpolated and non-interpolated probability density distributions for velocity gradients.

Figure 11 shows how well the values for $\overline{v_t^{2n}}$ and $\overline{v_*^{2n}}$ can be obtained for $2n=4$ and $2n=8$. Both integrals close reasonably well for the fourth-order moments. However, the very large scatter for $v_t^8\mathscr{P}^\dagger(v_t)$ at the larger values of v_t makes the eighth-order moments $\overline{v_t^8}$ less well defined. On the other hand, the values of $v_t^8\mathscr{P}^*(v_t)$ show much less scatter and $\overline{v_*^8}$ is rather well defined. It should be noted that the number of measured sample-points involved in determining the distribution of $v_t^4\mathscr{P}^\dagger(v_t)$ and $v_t^8\mathscr{P}^\dagger(v_t)$ in Figure 11 is 5 million and there is no reason a priori why the distribution of $v_t^8\mathscr{P}^\dagger(v_t)$ should necessarily be extended to much larger values of v_t; however, a question does arise as to whether, if more samples of data were used, the integrands $v_t^4\mathscr{P}^\dagger(v_t)$ and $v_t^8\mathscr{P}^\dagger(v_t)$ extend to further values of v_t. It is therefore desirable to evaluate the effect of this possibility on the measured data by making an appropriate extrapolation. It is in this context, as seen from Figure 11, that the interpolated distribution function $\mathscr{P}^*(v_t)$ can be used to best advantage, i.e., that due to the smaller scatter of the data it can be more appropriately extrapolated. The use of $\mathscr{P}^*(v_t)$ for that purpose is limited to determine the effect of the extrapolation and closure but not to determine the correct values for the moments $\overline{v_t^{2n}}$.

In order to increase the number of sample-recordings of data for evaluating measurements of higher-order moments from the closure point of view, 28 samples for the boundary-layer at $U_1=15.3$ m s^{-1} listed in Table II and used in Figure 7 were combined. Figure 12 shows how the averages for $\mathscr{P}^*(v_t)$ from the sample recordings compare for each separate experimental condition. It should be noted that 8 of the

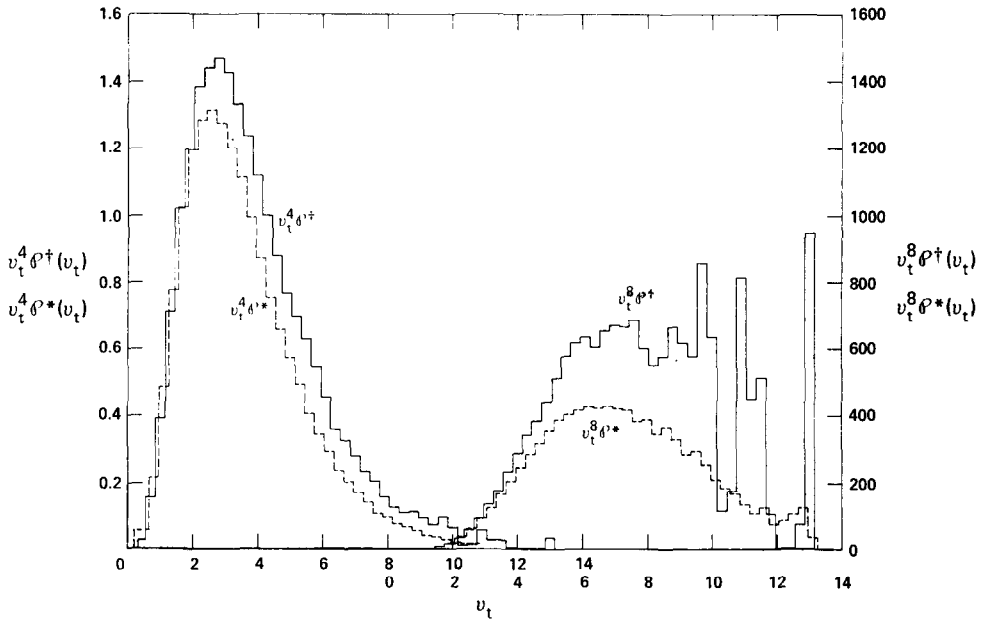

Fig. 11. Comparison of fourth- and eighth-order moments of the interpolated and non-interpolated probability density distributions.

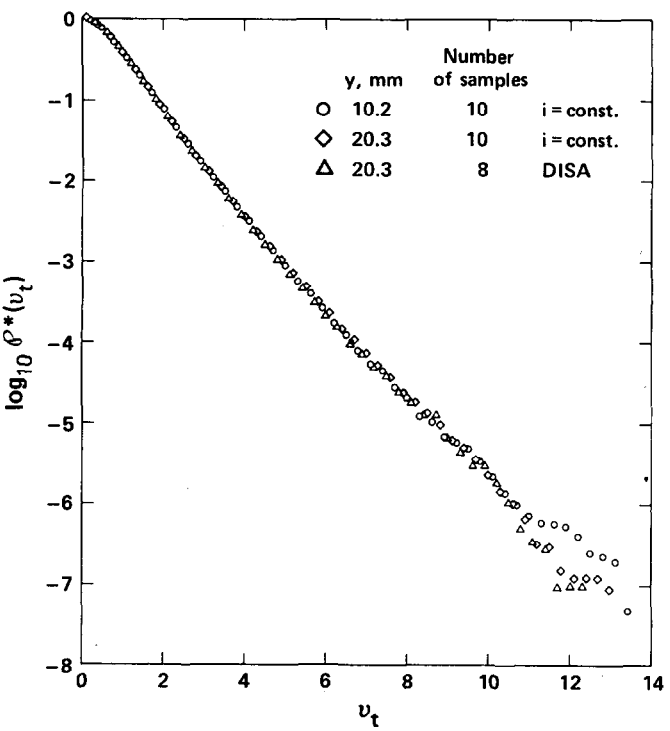

Fig. 12. Probability density distributions $\mathcal{P}^*(v_t)$ for different experimental conditions.

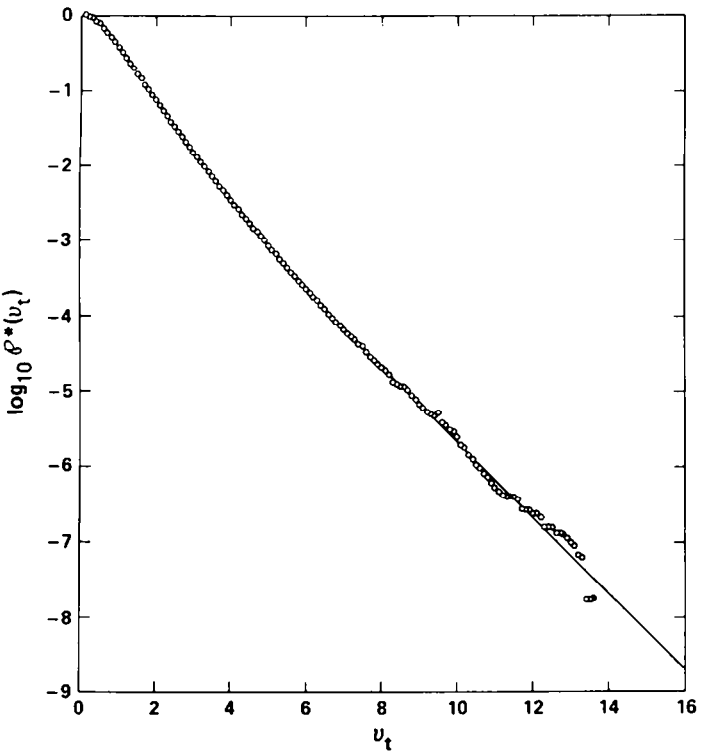

Fig. 13. Extrapolation of $\mathscr{P}^*(v_t)$ based on the average of 28 sample-recordings referred to in Figure 12.

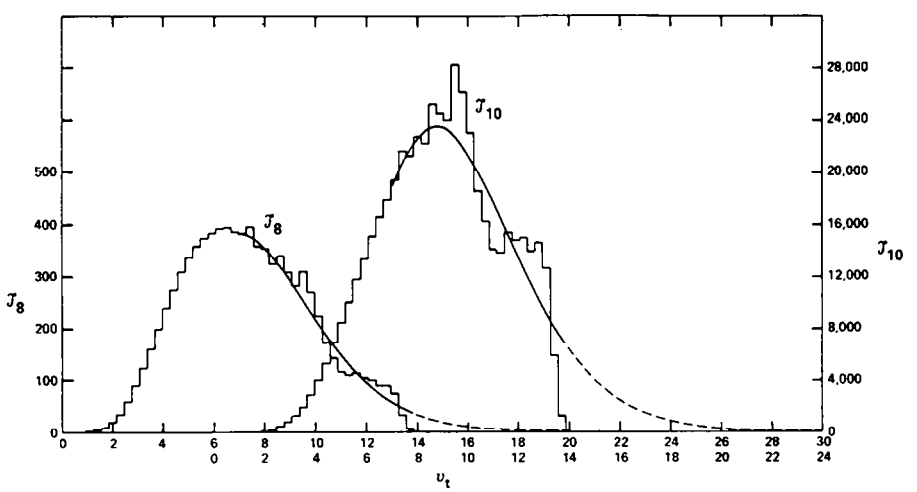

Fig. 14. Comparison of eighth- and tenth-order moments for extrapolated and non-extrapolated probability distributions $\mathscr{P}^*(v_t)$.

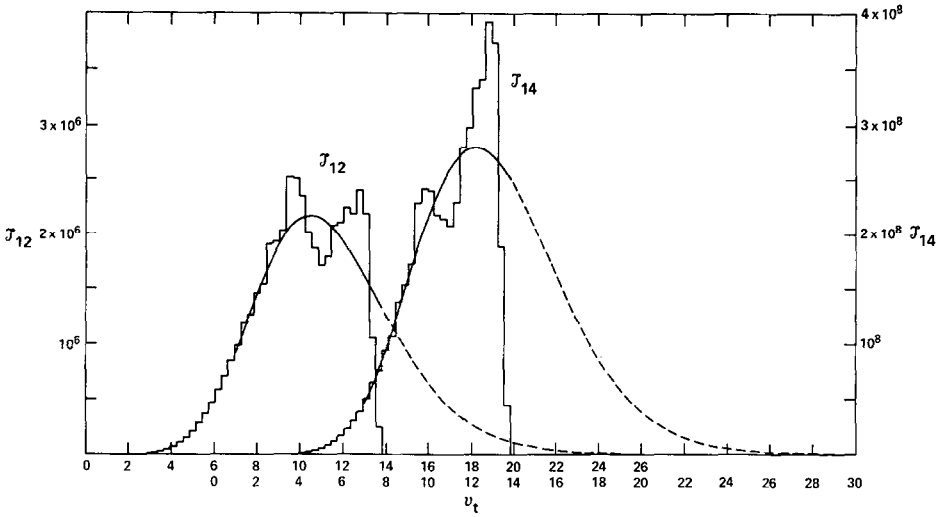

Fig. 15. Same as for Figure 14, but for the twelfth- and fourteenth-order moments.

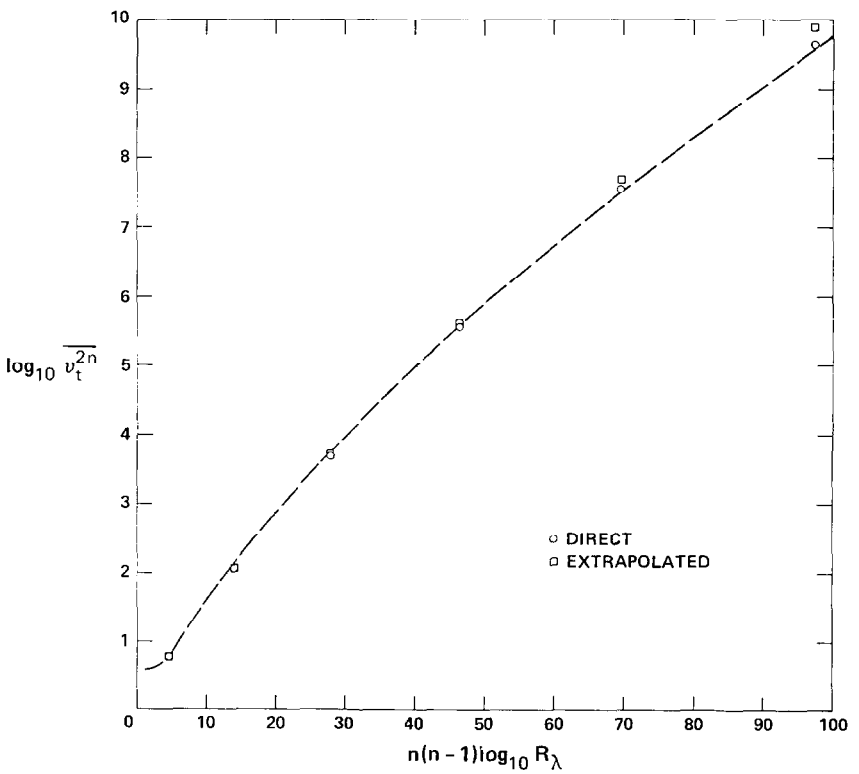

Fig. 16. Estimate of the effect of extrapolation of the probability density distribution on the higher-order moments.

sample-recordings were obtained with a constant-temperature linearized hot-wire anemometer and the two groups of 10 sample-recordings each were obtained with a constant current hot-wire anemometer illustrating again that the effect of non-linearity on the measurements of turbulent velocity gradients with the constant current anemometer is not significant. The agreement for the three groups of data provided an adequate justification for combining them. The resulting average for the 28 sample-recordings is shown in Figure 13. Also shown in Figure 13 is the exponential extrapolation to higher values of v_t which these data permit. Figures 14 and 15 compare the extrapolated data with the nonextrapolated data for

$$\mathscr{I}_n = v_t^{2n}\mathscr{P}^*(v_t)$$

with $2n=8$, 10, 12, and 14.

TABLE III

Ratio of extrapolated to non-extrapolated moments

$2n$	4	6	8	10	12	14
$(\overline{v_*^{2n}})_{\text{extr.}}/\overline{v_*^{2n}}$	1.0054	1.023	1.056	1.133	1.324	1.755

The ratios of the extrapolated moments $(\overline{v_*^{2n}})_{\text{extr.}}$ to the nonextrapolated moments $\overline{v_*^{2n}}$ are listed in Table III. The justification for applying the same ratios to the directly measured data for $\overline{v^{2n}}$ [as defined by Equation (1)] is given by Equation (13) which relates interpolated data for $\overline{v_*^m}$ to the directly measured $\overline{v^m}$. Implicit in this justification is the inference that Equation (13) is equally valid for the extrapolated case. For this purpose all the terms appearing in Equation (13) were directly measured for the 10 sample-recordings at $U_1=15.3$ m s^{-1} and $y=20.3$ mm for $\Delta t=0.025$ m s^{-1}. As seen from Table IV this relation is reasonably well satisfied.

TABLE IV

Comparison of values of $\overline{v_*^{2n}}$ obtained by two different methods

$2n$	2	4	6	8	10	12	14
From Equation (19)	0.9292	4.992	79.89	2770	162.2×10^3	13.36×10^6	1.367×10^9
From Equation (13)	0.9283	4.984	79.34	2693	150.7×10^3	11.61×10^6	1.103×10^9

Figure 16 shows the directly measured moments averaged over the 28 sample-recordings as well as those obtained by applying to the directly measured moments the appropriate extrapolation ratios given in Table III. The dashed curve is the same as the one given in Figure 7. It can be inferred from this comparison that the question of closure does not materially affect the conclusions previously drawn as to the deviation from lognormality and the departure from $\mu=$ const.

Another aspect which is involved in comparison with the theory is the consideration of the appropriate size of the average volume over which the measurements of v_t^2 should be made. This question has been, to some extent, evaluated by Chen (1971) and Gibson and Masiello (1972) using atmospheric data with inconsistent conclusions. Their procedure was to average sample values v_t^2 over an increasing number of time intervals Δt and then using the resulting averages to determine the probability distributions. Chen found a considerable improvement in the agreement of experimental data with the lognormal probability distribution. Gibson and Masiello, on the other hand, found that similar averaging had little effect on the range of lognormality of the probability distribution. In the context of the present paper, it is of interest to examine what effect such averaging would have on the conclusions drawn. Rather than proceed in a manner similar to Chen, and Gibson and Masiello, an indication as to whether the lack of appropriate averaging could account for the departure from $\mu = \text{const}$ can be readily obtained by a procedure similar to that illustrated in Figure 9. For this purpose, the average value of v_t^2 along the line AB is determined over the time interval Δt, namely

$$\widetilde{v_t^2(t)} = \frac{1}{\Delta t} \int_t^{t+\Delta t} v_t^2(t)\, \mathrm{d}t = v_*^2 . \tag{20}$$

Averaging over a large number of values for $(\tilde{v}_t^2)^n$ the higher order moments

$$\overline{(\tilde{v}_t^2)^n} = \overline{[\tfrac{1}{3}v_t^2(t) + \tfrac{1}{3}v_t(t)\, v_t(t+\Delta t) + \tfrac{1}{3}v_t^2(t+\Delta t)]^n} \tag{21}$$

are obtained, and the fourth-order moment, for example, is given by

$$\overline{(\tilde{v}_t^2)^2} = \tfrac{1}{9}[\overline{v_t^4(t)} + \overline{2v^3(t)\, v_t(t+\Delta t)} + \overline{3v_t^2(t)\, v_t^2(t+\Delta t)} + \\ + \overline{2v_t(t)\, v_t^3(t+\Delta t)} + \overline{v_t^4(t+\Delta t)}]. \tag{22}$$

Following this procedure, higher-order moments $\overline{(\tilde{v}_t^2)^n}$ for $n = 2$ to 7 were determined for one sample-recording at $U_1 = 15.3$ m s^{-1} and $y = 20.3$ mm. These are shown in Figure 17 for values of Δt ranging from 0 to 1.25 ms. After a very rapid change at small Δt, the various moments become approximately independent of Δt. Asymptotic values for large Δt (but relatively small as compared with the 12.5 s of the sample-recording) are obtained from Equation (21) assuming

$$\overline{v_t^{2n-k}(t)\, v_t^k(t+\Delta t)} = \overline{[v_t^{2n-k}(t)]}\, \overline{[v_t^k(t+\Delta t)]}$$

with $\overline{v_t} = 0$ and $\overline{v_t^2} = 1$. These are indicated by the dotted horizontal lines on the figure. It is of interest to note that Chen obtained averages for his dissipation rates for a time interval corresponding to 8 cm in length which is about 80 times the Kolmogoroff scale for the data which he used. The averaging times Δt in Figure 17 correspond to length averages from 3 to 150 Kolmogoroff scales. A $\Delta t = 6.75$ ms corresponds to the same ratio of averaging length to Kolmogoroff scale as Chen's.

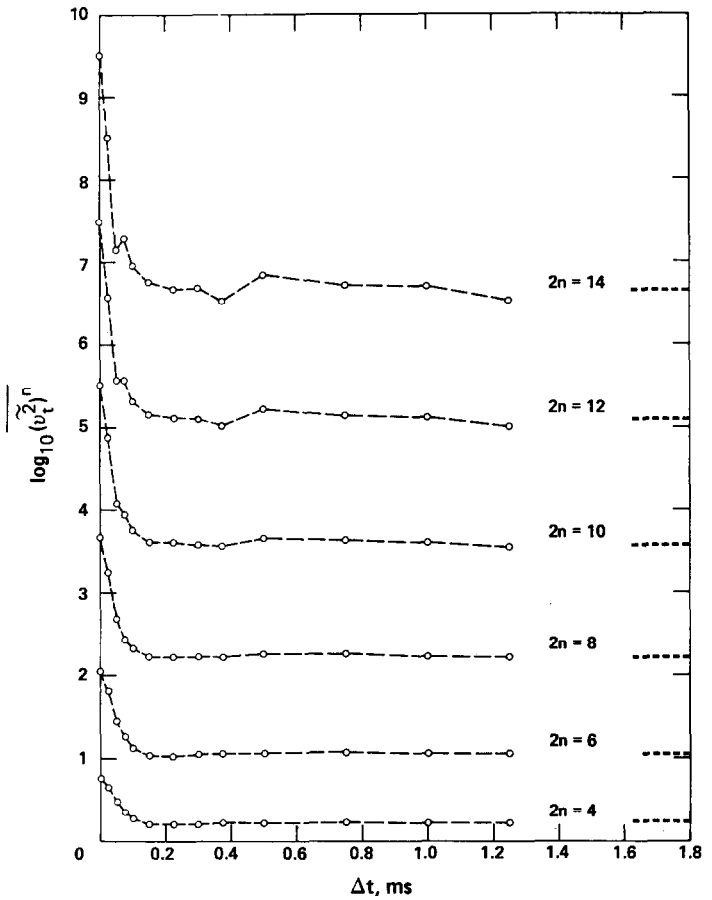

Fig. 17. The effect of increasing averaging time interval Δt on the measurements of higher-order moments.

The results obtained for $\overline{(\tilde{v}_t^2)^2}$ at various Δt are plotted in Figure 18 in a manner suggested by Equation (4). The value of the time-scale of turbulence

$$L_h = \int_0^\infty R(h)\,\mathrm{d}h,$$

where

$$R(h) = \frac{\overline{u(t)\,u(t+h)}}{\overline{u^2}}$$

was 2.61 ms (see Frenkiel and Klebanoff, 1973; Figure 6) and was selected as the macroscale. It is seen that only for a limited range of $L_h/\Delta t$ may the data be considered to follow a straight line as required by Equation (4). Similar behavior was observed

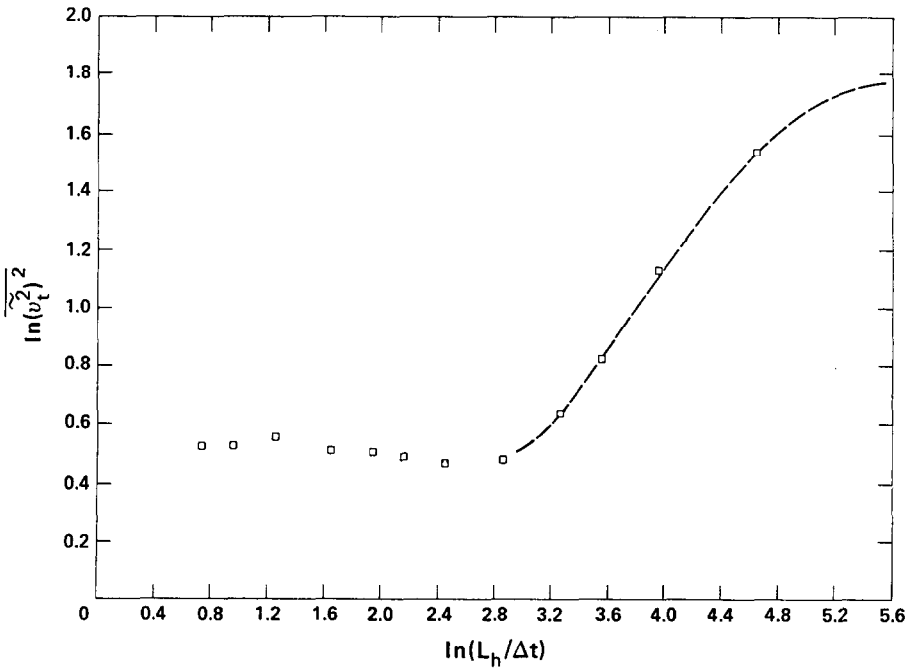

Fig. 18. Variation of fourth-order moments with nondimensional averaging time interval $L_h/\Delta t$.

by Gibson and Masiello although their scaling ratio and averaging procedure were different. From their data they inferred a value of $\mu=0.5$ while the value of μ corresponding to the straight line in Figure 18 is about 0.7. However, the significance of a value of μ inferred in this manner (from Figure 18) as shown in Figure 19 is questionnable. In Figure 19 higher-order moments $\overline{(\tilde{h}_t^2)^n}$ for $n=2$ to 7 are presented in a manner similar to that for $\overline{v_t^{2n}}$ in Figure 7 for various averaging time intervals Δt. The dashed curve corresponds to the curve in Figure 7. For values of Δt corresponding to the linear range of Figure 18 there is no evidence from the measurements of higher-order moments of $\mu=$ const. In fact, the effect of increased averaging time interval is in the opposite direction.

5. Conclusions

It is noted that, using appropriate numerical methods of improving precision, relatively reliable values can be obtained for higher-order moments of turbulent velocity gradients. Measurements of such moments in the nearly isotropic turbulent field generated by a grid and in the boundary-layer of a plate have demonstrated that they correlate in a form related to lognormality of the probability of the dissipation, but do not conform to the requirement imposed by lognormality of a constant μ. It is

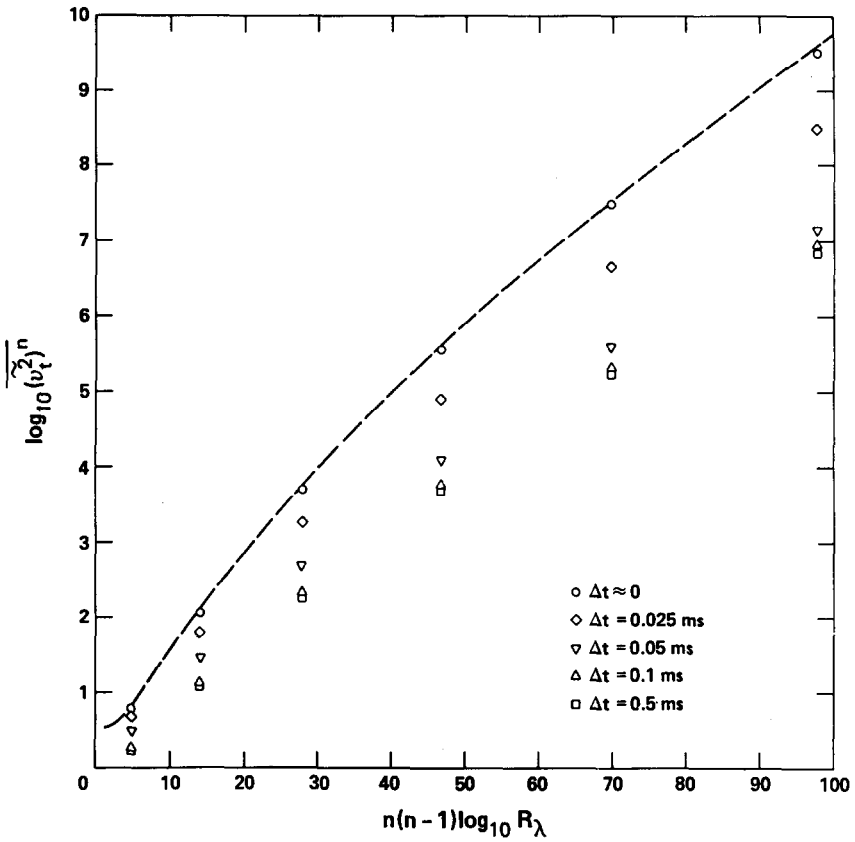

Fig. 19. Higher-order moments obtained for several averaging time intervals Δt in a form suggested by lognormality.

also demonstrated that it is reasonable to infer that the existing atmospheric data can be considered to be consistent with measurements made in a laboratory and that the fact that μ is not constant may not necessarily be due to an insufficiently large Reynolds number of turbulence.

Acknowledgements

The authors wish to express their gratitude to K. D. Tidstrom and to L. M. Sargent for their assistance in the recording of analog data and the hot-wire instrumentation; to Mrs Dolores R. Wallace and J. B. Moulton for their aid in computer programming and computing; to R. B. Johnson, Jr. and G. P. Marques for their assistance in digitizing.

This work was performed with the partial support of the Division of Biology and Medicine of the U.S. Atomic Energy Commission.

References

Antonia, R. A.: 1973, 'Some Small Scale Properties of Boundary Layer Turbulence', *Phys. Fluids* **16**, 1198–1206.

Batchelor, G. K. and Townsend, A. A.: 1949, 'The Nature of Turbulent Motion at Large Wave-Numbers', *Proc. Roy. Soc.* **A199**, 238–255.

Chen, W. Y.: 1971, 'Lognormality of Small-Scale Structure of Turbulence', *Phys. Fluids* **14**, 1639–1647.

Comte-Bellot, G.: 1965, *Ecoulement turbulent entre deux parois parallèles*, Publ. Sci. et Tech. du Min. de l'Air, Paris.

Corrsin, S.: 1962, 'Turbulent Dissipation Fluctuations', *Phys. Fluids* **5**, 1301–1302.

Corrsin, S. and Kistler, A. L.: 1954, 'The Free-Stream Boundaries of Turbulent Flows', NACA Technical Note 3133.

Frenkiel, F. N.: 1952, 'The Comparison Between the Longitudinal Correlation and the Time Correlation in a Turbulent Flow', *Phys. Rev.* **88**, 1380–1382.

Frenkiel, F. N. and Klebanoff, P. S.: 1965, 'Two-Dimensional Probability Distribution in a Turbulent Field', *Phys. Fluids* **8**, 2291–2293.

Frenkiel, F. N. and Klebanoff, P. S.: 1967, 'Higher-Order Correlations in a Turbulent Field', *Phys. Fluids* **10**, 507–520.

Frenkiel, F. N. and Klebanoff, P. S.: 1971, 'Statistical Properties of Velocity Derivatives in a Turbulent Field', *J. Fluid Mech.* **48**, 183–208.

Frenkiel, F. N. and Klebanoff, P. S.: 1973, 'Probability Distributions and Correlations in a Turbulent Boundary Layer', *Phys. Fluids* **16**, 725–737.

Gibson, C. H. and Masiello, P. J.: 1972, 'Observations of the Variability of Dissipation Rates of Turbulent Velocity and Temperature Fields', in M. Rosenblatt and C. Van Atta (eds.), *Statistical Models and Turbulence*, pp. 427–453, Springer-Verlag.

Gibson, C. H., Stegen, G. R., and McConnell, S.: 1970, 'Measurements of the Universal Constant in Kolmogoroff's Third Hypothesis for High Reynolds Number', *Phys. Fluids* **13**, 2448–2451.

Gurvich, A. S. and Yaglom, A. M.: 1967, 'Breakdown of Eddies and Probability Distributions for Small-Scale Turbulence', *Phys. Fluids Suppl.* **10**, S59–S65.

Gurvich, A. S. and Zubkovskii, S. L.: 1963, *Izv. Akad. Nauk SSSR, Ser. Geofiz* **12**, 1856.

Klebanoff, P. S.: 1954, 'Characteristics of Turbulence in a Boundary-Layer with Zero Pressure Gradient', NACA Technical Note 3178; also 1955, NACA Report 1247.

Klebanoff, P. S. and Diehl, Z. W.: 1951, 'Some Features of Artificially Thickened Fully Developed Turbulent Boundary Layers with Zero Pressure Gradient', NACA Technical Note 2475; also 1952, NACA Report 1110.

Kline, S. J., Morkovin, M. V., Sovran, G., and Cockrell, D. J. (eds.): 1969, *Proceedings of the Computation of Turbulent Boundary–Layers – 1968*, AFOSR-IFP-Stanford Conference, Stanford University.

Kolmogoroff, A. N.: 1962, 'A Refinement of Previous Hypothesis Concerning the Local Structure of Turbulence in a Viscous Incompressible Fluid at High Reynolds Number', in *Mécanique de la Turbulence*, Centre National de la Recherche Scientifique, Paris, pp. 447–458; also 1962, *J. Fluid Mech.* **13**, 82–85.

Kuo, A. Y. and Corrsin, S.: 1971, 'Experiments on Internal Intermittency and Fine-Structure Distribution Functions in Fully Turbulent Fluid', *J. Fluid Mech.* **50**, 285–320.

Obukhov, A. M.: 1962, 'Some Specific Features of Atmospheric Turbulence' *J. Geophys. Res.* **67**, 3011–3014; also 1962, *J. Fluid Mech.* **13**, 77–81.

Orszag, S. A.: 1970, 'Indeterminacy of the Moment Problem for Intermittent Turbulence', *Phys. Fluids* **13**, 2211–2212.

Pond, S. and Stewart, R. W.: 1965, *Izv. Atmos. Ocean. Phys.* **1**, 914.

Sheih, C. M., Tennekes, H., and Lumley, J. L.: 1971, 'Airborne Hot-Wire Measurements of the Small-Scale Structure of Atmospheric Turbulence', *Phys. Fluids* **14**, 201–215.

Stewart, R. W., Wilson, J. R., and Burling, R. W.: 1970, 'Some Statistical Properties of Small Scale Turbulence in an Atmospheric Boundary-Layer', *J. Fluid Mech.* **41**, 141–152.

Tennekes, H.: 1968, 'Simple Model for the Small-Scale Structure of Turbulence', *Phys. Fluids* **11**, 669–671.

Tennekes, H. and Wyngaard, J. C.: 1972, 'The Intermittent Small-Scale Structure of Turbulence: Data Processing Hazards', *J. Fluid Mech.* **55**, 93–103.

Van Atta, C. W. and Chen, W. Y.: 1968, 'Correlation Measurements in Grid Turbulence Using Digital Harmonic Analysis', *J. Fluid Mech.* **34**, 497–515.

Wygnanski, I. and Fiedler, H. E.: 1970, 'The Two-Dimensional Mixing Region', *J. Fluid Mech.* **41**, 327–361.

Wyngaard, J. C.: 1968, 'Measurements of Small-Scale Turbulence Structure with Hot Wires', *J. Sci. Instrum. (J. Phys. E)* **1**, 1105–1108.

Wyngaard, J. C. and Tennekes, H.: 1970, 'Measurements of the Small-Scale Structure of Turbulence at Moderate Reynolds Numbers', *Phys. Fluids* **13**, 1962–1969.

Yaglom, A. M.: 1966, 'The Influence of Fluctuations in Energy Dissipation of the Shape of Turbulence Characteristics in the Inertial Interval', *Dokl. Akad. Nauk SSSR* **166**, 49–52 (English translation: 1966, *Sov. Phys.-Dokl.* **11**, 26–29).